Coastal Dynamics 2017
Paper No. 087

MORPHODYNAMIC EVOLUTION OF PLANE BEACH UNDER PURE TIDAL CURRENT

Van Huynh[1], Nicholas Dodd[2], Fangfang Zhu[3]

Abstract

We calculate both bed load and suspended load transport under cross-shore tidal currents on an intertidal zone of a macro-tidal beach. Our method employs the shallow-water equations coupled to an advection equation for suspended concentration and bed evolution equation. The physical domain including the shoreline is mapped onto fixed computational domain. This method allows the results to be obtained readily throughout the whole domain over long simulations. The morphodynamics of a plane macro-tidal flats comprising fine and medium sand is considered. Under cross-shore tidal currents, the convex upward profile builds up in the intertidal region; while the lower parts below the low tide level tend to retreat over time. The shoreward movement of sediment is more likely due to suspended-load rather than bed-load. We then consider an erosional formula based on linear wave theory in order to take into account the entrainment due to waves. The bed change with respect to this erosional term is obtained over one tidal cycle. Further work is under way to correctly characterise differences in wave and current effects.

Key words: numerical models; shallow water; coupled hydro-morphodynamic model; coordinate transformation method; non-breaking long waves, tidal waves

1. Introduction

Tidal flats are characterised by varying water depths both temporally and spatially. The variations in water level are likely to generate specific hydrodynamics, which associate with sediment transport processes. The hydrodynamics are responsible for generating bed shear stresses and mobilising sediment, which can be advected by the flow, and may subsequently be deposited. These main hydrodynamic forcings are described by Eisma (1997), including tide, waves, the wind-induced circulation, the density-driven circulation and the drainage process.

Assessing how all of these processes contribute to the bed stress is complicated, especially at extremely shallow water depths, where the validity of the bottom shear stress approximation is questionable. As shown by Friedrichs and Aubrey (1996), the hydrodynamics and morphodynamics are interrelated. Their analytical study focused upon the dependence of flows or waves on the equilibrium topography, which has been confirmed numerically by Roberts et al. (2000). The simplified numerical model was developed to analyse interactions between hydrodynamics and sediment transport, and thus the possible equilibrium profiles.

For the intertidal zone, bed irregularities are more likely controlled long-term by the combination of a variety of factors, including tidal range, wave climate, sediment properties, sediment supply, bed gradient and tidal currents (Masselink and Short, 1993). Le Hir et al. (2000) indicated that long-term morphologies of intertidal flats are driven dominantly by tides. Kirby (2000) also found that over a long-term timescale (decadal time scale), wave-dominated flats are concave-upward profile and retreating, while tide-dominated are convex-upward and accreting (Fig. 1). In both types of flats, tide is a crucial factor, as its periodic submerging and exposing on these flats defines the intertidal region. Moreover, hydrodynamics on tidal flats are strongly correlated with this periodic variation: onshore tidal current during rising tides and offshore current during falling tides. Tidal currents can be split into a cross-shore component, which accounts for the periodic fluctuation of mean water level of the flat, and a long-shore component, which depends on the large-scale circulation around the flat. On beaches subjected to large tidal ranges (>3m), the

[1] Department of Civil Engineering, University of Nottingham, UK. van.huynh@nottingham.ac.uk
[2] Department of Civil Engineering, University of Nottingham, UK. nicholas.dodd@nottingham.ac.uk
[3] University of Nottingham, Ningbo, China, 315100. fangfang.zhu@nottingham.edu.cn

induced tidal currents are even more complicated. The relative magnitude of these two components depends on the local geological and hydrodynamic settings. Cross-shore currents tend to be dominant where the tidal flat gradient is low or where the presence of a headland, spit, or breakwater reduces the long-shore component (Roberts et al., 2000). At these intertidal flats, the cross-shore component is usually considered as a dominant factor, which is responsible for the mobilisation of sediment.

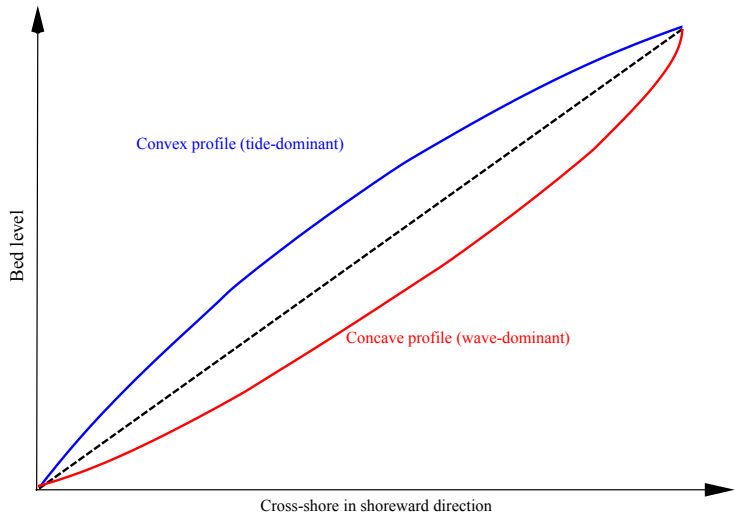

Figure 1. Equilibrium profile of tide- and wave- dominant tidal flats

Waves, either due to swell or generated by local winds, also contribute to the entrainment of suspended sediment on shallow tidal flats (Green and Coco, 2013). Even in sheltered areas, waves are seldomly negligible, as small waves can sufficiently re-suspend sediments in very shallow areas, and often contribute to morphological stability in the long-term (Le Hir et al., 2000). In the case of most UK tidal flats, wave height is insignificant compared to the tidal range, which means the waves induce a band of high shear stress which moves across the tidal flats with tide variation (Roberts et al., 2000). Li and Mehta (1997) suggested that waves contribute to sediment transport in these flats by two main mechanisms: raising the entrainment rate by increasing bed shear stresses, which is the advected; and fluidisation or liquefaction of the top layer of bed, which is then carried seawards/shorewards under gravity/wave-induced residual currents.

Over the past decade, increasing efforts have been made to investigate cross-shore morphology of tidal flats. Friedrichs and Aubrey (1996) assumed that the maximum bed shear stress is uniform spatially with uniform current speeds, and derived analytical solutions of equilibrium profiles of tidal flats where sediment is transported under tide- or wave-dominated regimes. The main findings were also confirmed by Kirby (2000) and Roberts et al. (2000) that the convex and concave shape of tidal flats are experienced at tide- and wave-dominated flats, respectively. Extending the numerical model of Roberts et al. (2000), Pritchard et al. (2002) and Pritchard and Hogg (2003a) investigated the long-term morphodynamic behaviour of tide-dominated mudflats under different tidal and sediment supply conditions. The main finding was that cross-shore accretion does not depend on the tidal range but the sediment supply. The role of these mechanisms either in isolation (Pritchard and Hogg, 2003a; Friedrichs and Aubrey, 1996) or in conjunction with each other (Robert et al., 2000) are less well understood because of the greater complexity of the hydrodynamics. In the past decade, increasing efforts have been attempted to investigate the morphology of tidal flats, primarily focusing on cohesive sediment with the suspended-load only. For non-cohesive sediment, the bed-load transport becomes more important and also contributes significantly to the morphodynamics of tidal flats. In this paper, we, however, are concerned with tidal flats that evolve under pure tidal forcing in which both bed load and suspended load transport are considered. This idealisation allows the identification of environmental factors which exert most influences on the evolution of tidal flats and thus characterise the morphodynamics under certain conditions.

2. Description of the model

Our main interest is macro-tidal flats which are common in the UK, and the physical parameters reflecting these areas. Le Hir et al. (2000) indicated that long-shore currents are likely to dominate the sediment transport only in deeper water. Thus, we consider cross-shore tidal currents as the main forcing hydrodynamic. Hydrodynamics in a shallow water region such as the nearshore zone can be well described by the nonlinear shallow water equations. These equations characterise well the water motion in which the velocity can be considered as depth-invariant. In simplifying but still adequately describing the fundamental physical phenomena, and thereby allowing a more rapid numerical solution, the NSWEs possess distinct advantages over more comprehensive equations sets, such as the Euler equations, for modelling long waves such as waves in the swash and inner surf zones and tidal motions:

$$\hat{h}_{\hat{t}} + \left(\hat{h}\hat{u}\right)_{\hat{x}} = 0 \tag{1}$$

$$\hat{u}_{\hat{t}} + \hat{u}\hat{u}_{\hat{x}} + g\hat{\eta}_{\hat{x}} = -\frac{\tau_b}{\rho\hat{h}} \tag{2}$$

where $\hat{h}$ is the water depth, $\hat{u}$ is the depth-averaged velocity, $\hat{\eta}$ is the water surface elevation and τ_b is the bed shear stress. From the hydrodynamics, the transport of suspended sediment is found from an advection equation of suspended sediment with erosion and deposition terms included.

$$\hat{c}_{\hat{t}} + \hat{u}\hat{c}_{\hat{x}} = \frac{\hat{E}-\hat{D}}{\hat{h}} \tag{3}$$

where $\hat{c}$ is the depth-averaged concentration, $\hat{E}$ is the flux of sediment from the bed into suspension by erosion and $\hat{D}$ is the flux of suspended sediment onto the bed by deposition. $\hat{E}$ and $\hat{D}$ are evaluated by

$$\hat{E} = \begin{cases} \widehat{m_e}\left(\frac{\tau_b}{\tau_{s,cr}} - 1\right) & \text{for } \tau_b \geq \tau_{s,cr} \\ 0 & \text{for } \tau_b < \tau_{s,cr} \end{cases} \tag{4}$$

$$\hat{D} = \widehat{\omega_s}\hat{c} \tag{5}$$

where $\widehat{m_e}$ is a parameter related to rate of entrainment of sediment into water column, $\hat{\tau}_{s,cr}$ is suspended-load sediment critical bed shear stress at which the sediment is eroded into the water column, and $\widehat{\omega_s}$ is the settling velocity of suspended sediment. However, it is noted that the entrainment given in (4) is due to tidal motion, which is, in fact, very insignificant compared to the entrainment due to wave. In our model, although we do not consider sediment transport due to wave-generated currents, the entrainment flux caused by breaking waves is taken in to account and considered as the only entrainment mechanism. During propagation, waves may break on shallow tidal flats because of the growth of wave steepness. The wave-induced bed shear stress achieves its maximum value at breaking point and reduces landward (Green and Coco, 2013).

The wetting and drying at the shoreline are treated by coordinate transformation method so that the physical domain (x, t) is mapped onto a new computational domain $(\bar{x}, \bar{t})$ without including the dry cells (Huynh et al., 2017). A sinusoidal variation in water level is imposed as tidal variation at the boundary. The bed change equation is coupled with hydrodynamics and updated at each hydrodynamic time step.

$$\hat{B}_{\hat{t}} + \xi(\widehat{q_b})_{\hat{x}} = \xi(\hat{D} - \hat{E}) \tag{6}$$

where $\widehat{q_b}$ is bed load sediment flux determined by Meyer-Peter and Müller formula, $\xi = 1/(1-p)$, where p is the bed porosity. Following the transformation method and nondimensionalisation given in Huynh et al. (2017), the governing equations (1), (2), (3) and (6) become

$$h_{\bar{t}} + A_1 h_{\bar{x}} + A_2 (hu)_{\bar{x}} = 0 \tag{7}$$

$$u_{\bar{t}} + A_1 u_{\bar{x}} + A_2(uu_{\bar{x}} + h_{\bar{x}} + B_{\bar{x}}) = -c_D \frac{|u|u}{h} \quad (8)$$

$$c_{\bar{t}} + A_1 c_{\bar{x}} + A_2 u c_{\bar{x}} = \frac{\tilde{E}(u^2 - c)}{h} \quad (9)$$

$$B_{\bar{t}} + A_1 B_{\bar{x}} + 3A_2 \sigma u^2 u_{\bar{x}} = M(c - u^2) \quad (10)$$

where $\tilde{E} = (\widehat{\omega_s}/\sqrt{(g\hat{h}})$. It should be noted that $\tilde{E} = E \tan\alpha$, where E is the exchange rate parameter of Pritchard and Hogg (2005), which is representative of the settling velocity of sediment. $M(\sigma)$ is dimensionless bed mobility with respect to suspended load (bed load). C_D is friction coefficient.

3. Model verification test

The model is firstly tested using the same schematic configuration that was adopted by Pritchard and Hogg (2003b) (PH03)

3.1. *Model Setup*

The suspended sediment transport under reflected long waves forcing at infragravity frequencies on a plane beach was obtained analytically by PH03. They employed the nonlinear shallow water equations coupled with the advection of suspended sediment concentration in Lagrangian coordinates. The suspended sediment transport under such waves is localised close to the shoreline and principally directed landward, which is not responsible for the tendency of wave-dominated tidal flats to erode sediment over the long-term. However, their findings provided a useful test case against which to validate our model.

It is also noted that the entrainment and deposition fluxes in (4) and (5) have been here adapted to include the deposition of flocs (see Pritchard and Hogg, 2003b for details). We consider a plane beach with domain length of $L = 100$ and gradient of $1/100$. Long low-frequency waves with period of $T = \pi$ and $H = 0.02$ is specified at the offshore boundary. These nondimensional parameters are consistent with the reference values applied by PH03 (see section 2.1.1. in Pritchard and Hogg, 2003b). The hydrodynamic under these parameter is also consistent with the analytical periodic results of $A = 0.2$ and $\omega = 1$ suggested by Carrier and Greenspan (1958). $\xi = 0$ is used to prevent any bed change to occur. This is consistent with the fixed bed condition used in PH03.

3.2. *Concentration field and net fluxes over time*

It is found that regardless of the initial condition for suspended sediment, the concentration field achieves a periodic state after a few cycles. The concentration field is spatially localised, and most apparently in the very nearshore region. It means that under the conditions of long low-frequency waves, velocities are high enough to entrain sediment only in the nearshore region. This is correlated with the high concentration field observed at these positions. The results of periodic concentration field are shown in Fig. 2, while the instantaneous and net cross-shore sediment flux are shown in Fig. 3 and Fig. 4 respectively.

The results are in good agreement as can be seen in three figures. The settling and scour lag are easily visualised as shoreline solutions of c and u in Fig. 4. The delayed response of the concentration field to the variation in the velocity is observed. It is noted that the hydrodynamics in the model are driven by a sinusoidal signal at the offshore boundary instead of the Carrier and Greenspan (1958) analytical solutions. Thus, there are some small discrepancies in hydrodynamic solutions comparing to Pritchard and Hogg (2003b) (Huynh et al., 2017). This principally explain the small difference between our model and reference results and may indicate why the net flux $Q(x)$ is higher erosion seaward but less accretion shoreward (Fig. 4). The performances of the present model are also confirmed against other numerical models in both hydrodynamics and morphodynamics with good agreement (Huynh et al., 2017). It suggests that this coupled model is suitable for prediction of the morphodynamic evolution of a non-cohesive bed

under the influence of long waves such as tidal currents.

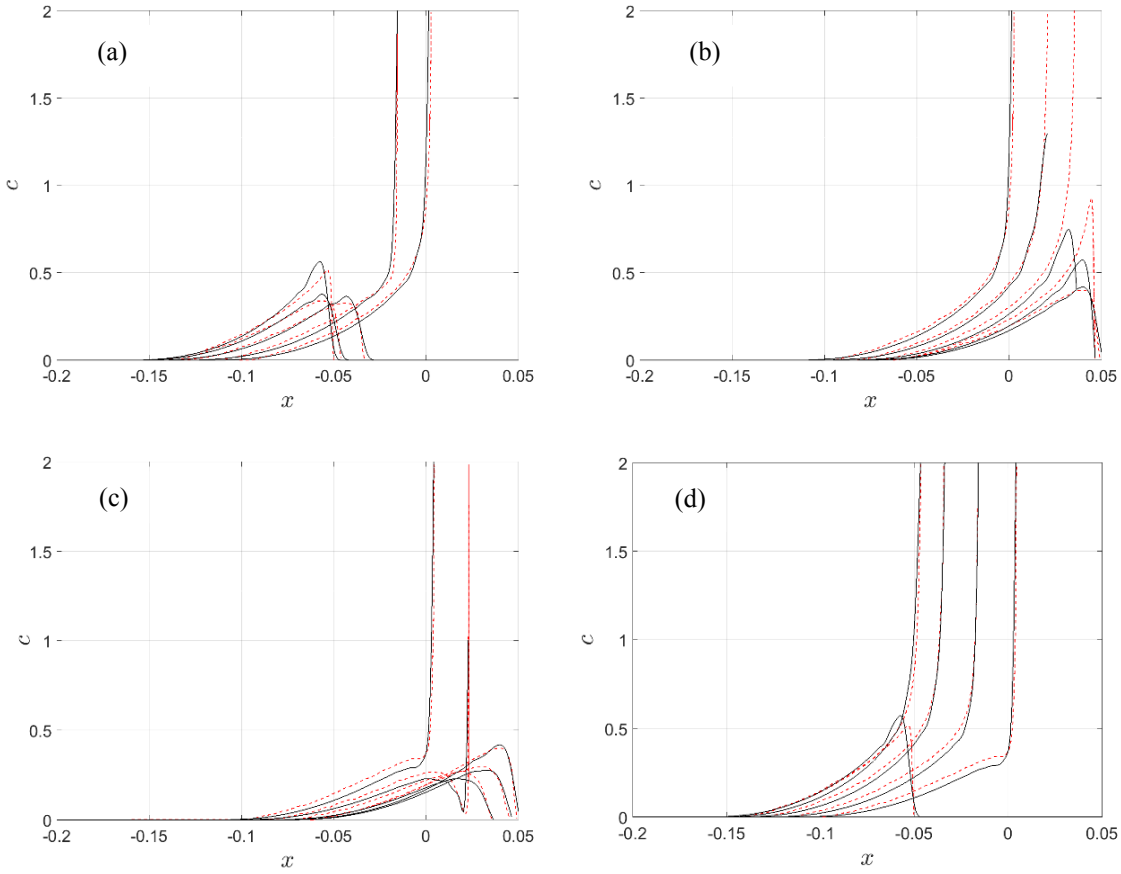

Figure 2. Suspended concentration under PH03 flow conditions: plot at intervals of $\pi/16$. (a) first half of run-up; (b) second half of run-up; (c) first half of run-down; (d) second half of run-down (PH03 solutions: red dashed, present solutions: black solid)

4. Morphodynamic evolution under tidal currents only

In this section, we aim to investigate the effects morphology evolution under the influence of tidal currents only. We consider a rather gently sloping flat associated with tide-dominated tidal flats (Short, 1991) with gradient of 0.005 and initial domain length at mid-tide of 2km. The hydrodynamics is driven at the offshore boundary by a semidiurnal sinusoidal signal of 5m tidal range. For sand of the median grain size of $D_{50} = 0.2$mm, typical values of sediment properties are given in Table 1 (Soulsby, 1997). For the given bathymetry and physical parameters, the corresponding dimensionless parameters are $\tilde{E} = 2\times10^{-3}$; $M = 2\times10^{-4}$ and $\sigma = 2\times10^{-4}$. The effects of bed- and suspended-load (relating to suspended concentration) on bed evolution are represented by σ, M (and $\tilde{E}$), respectively. Following Huynh et al. (2017), these parameters are related to sediment properties. It is noted that these parameters are significantly smaller than those applied in swash event, where the hydrodynamic is much more dynamical (Zhu and Dodd, 2015). By considering a broad range of parameters on a same bed bathymetry, we can examine the morphodynamics of different bed sediment and investigate the effect of individual and combined load mode on the final bed change.

Table 1. Typical physical parameters associated with fine sand sediment

$\widehat{m_e}$	1×10^{-3}	m/s
$\widehat{\omega_s}$	2×10^{-2}	m/s
ρ	1027	kg/m^3
$\tau_{s,cr}$	0.2	N/m^2
C_D	4×10^{-3}	
p	0.5	

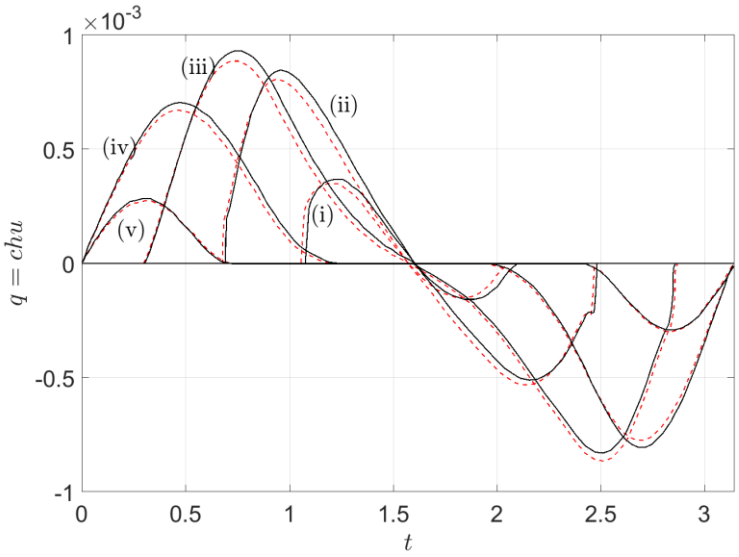

Figure 3. Instantaneous sediment flux $q(x,t)$ over a period obtained at: (i) $x = 0.0325$; (ii) $x = -0.0025$; (iii) $x = -0.0375$; (iv) $x = -0.0725$; $x = -0.1075$ (PH03 solutions: red dashed, present solutions: black solid)

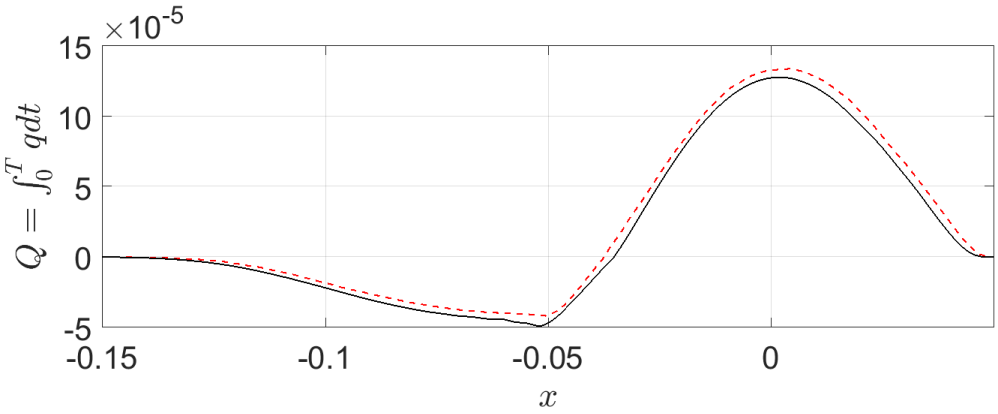

Figure 4. Net flux $Q(x)$ over a period (PH03 solutions: red dashed, present solutions: black solid)

4.1. Combined mode of load transport

The parameters σ, M and $\tilde{E}$ evaluated above are used as reference values. The bed profile and bed change after 500 tidal periods under combination of bed and suspended-load transport are shown in Fig. 5. The behaviour of non-cohesive sediment morphodynamics under tidal currents is similar to muddy sediment in the previous studies (Kirby, 2000 and Roberts et al., 2000). There is a tendency of shoreward transport of

net sediment under tidal currents. The accretion in the intertidal zone continues with time until an equilibrium convex-upward profile in the intertidal zone is achieved. At the lower part of the tidal flat region where the bed is always submerged below water level, erosion is observed. Because of the conservation in sediment, this erosional sediment is supposed to be carried shoreward under tidal currents and accrete in the intertidal zone.

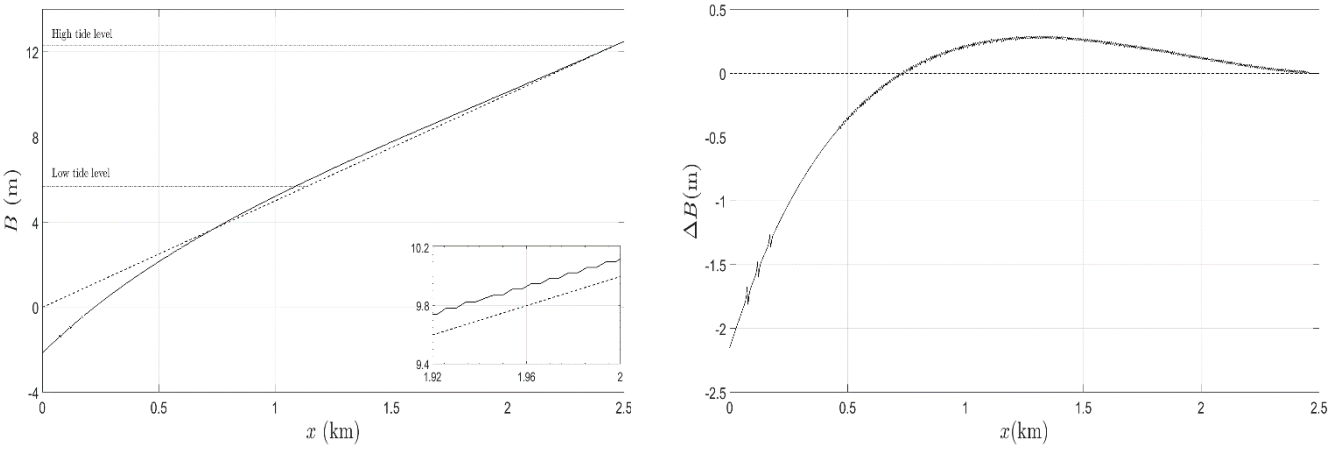

Figure 5. Bed profile B (left) and bed change ΔB (right) versus cross-shore distance x after 500 tides for combined mode

4.2. Bed-load transport only and suspended-load transport only

Bed change under bed-load transport only is achieved by setting $M = 0$ in the model. The final bed changes after 500 tidal periods for various $\sigma = 2\times10^{-4}$, 2×10^{-3} in comparison with above reference solutions are shown in Fig. 6. $M = 0$ means there is no entrainment of sediment into water column (Huynh et al., 2017), thus c is locally controlled by velocity field, exchange rate parameter and pre-suspended sediment. Since the equilibrium state is set initially, there is neither erosion nor deposition throughout the domain. It is noted that this is instantaneous equilibrium, which vary locally. Since there is no entrainment, sediment settles down and c quickly approaches zero. c will remain zero no matter how the value of $\tilde{E}$ varies.

Similarly, setting $\sigma = 0$ means there is no bed mobility with respect to bed-load transport; the sediment transportation takes place by suspended-load transport only. The final bed changes under this transportation mode with $M = 2\times10^{-4}$ and 2×10^{-3} are shown in Fig. 6. It can be seen from Fig.6 that the bed change due to bed-load only tend to erode, while those due to suspended-load accrete over time with the effects are significant at the lower part of tidal flats.

The patterns of bed change due to bed load only are quite similar for varous values of σ. It is also noticed that there are erosions due to bed-load transport occurring at the lower part. However, small accretions are still observed in the upper part with varied σ. The suspended-load transport tends to move the sediment shoreward and build up profile at the intertidal zone. Regarding suspended-load only, increasing M does not seem to increase the magnitude of accretion but is likely to shift the accretion more shoreward (Fig. 6). It is noted that the similar tendency of moving the suspended cohesive sediment shoreward was also observed by Pritchard and Hogg (2003a). Considering the bed change in intertidal zone by varying both σ and M, it appears that the shoreward movement of sediment is likely due to the suspended-load rather than due to bed-load.

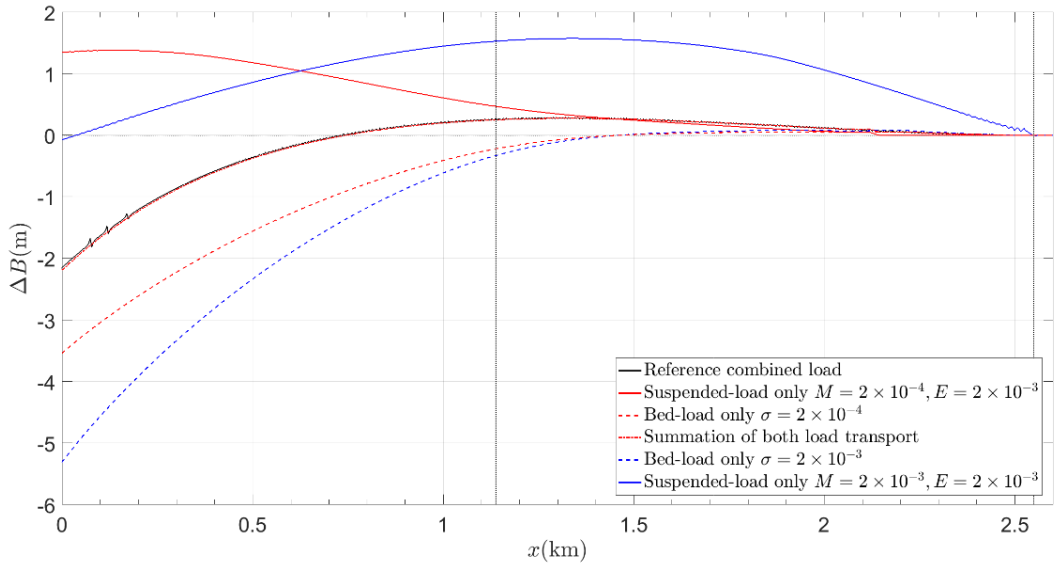

Figure 6. Bed change ΔB due to different transport type versus cross-shore distance x (black solid line: reference bed change in §4.1, two vertical dotted lines represent positions of low and high tide)

5. Development for wave-generated entrainment and erosional flux

As mentioned in §4, suspended load is the dominant factor in the morphodynamics of intertidal region. However, tide is not the only factor to contribute to sediment suspension in the surf zone. Wind-waves have a typically short period compared to tides, but in shallow water the wave-orbital motions are very likely to penetrate down to the bottom and resuspend sediments in intertidal zone. Orbital motions of even very small waves height (less than 20cm) are able to resuspend intertidal flat sediments (Anderson, 1972; Green, 2011). In some intertidal flats with low tidal range, tidal currents are incapable of resuspending sediments, and the entrainment of sediment into the water column is mainly controlled by waves (Green et al., 1997). In this model, instead of the erosion source term given in (4), we employ different equations which take into account erosion due to waves.

The ratio of wind-wave wavelength to water depth varies significantly, leading to the variation in wave-orbital speed and wave-induced bed shear stress. In this model, we assume that the incident wave conditions at offshore boundary is constant over a tide. Thus, water depth is a main control on the wave-induced bed shear stress, and associated entrainment flux. The wave-induced bed shear stress achieves its maximum once breaking occurs and reduces shoreward with water depth (Green and Coco, 2013). We assume that the entrainment of suspended sediment only takes place when waves start to break. A breaking index of $\gamma_b = 0.5$ is considered following Roberts et al. (2000). For a given wind-wave incident at seaward boundary of wave height H and period T, the wave-orbital velocity amplitude at sea bed is given by linear wave theory as

$$u_{w,b} = \frac{\pi H}{T \sinh(kh)} \tag{11}$$

where k is the wave number. Under waves-only condition (i.e., without tidal current), the associated wave-induced bed shear stress τ_w is obtained using a quadratic bottom friction

$$\tau_w = \frac{1}{2} \rho f_w u_{w,b}^2 \tag{12}$$

$$f_w = 1.39\left[\frac{u_{w,b}T}{2\pi(D_{50}/12)}\right]^{-0.52} \quad (13)$$

where f_w is the wave friction factor, following Soulsby (1997) and D_{50} is the median grainsize of the bed sediment. Roberts et al. (2000) assumed a linear summation for the total bed shear stress from tidal currents and waves. In our model, the bed shear stress is assumed to be influenced by wave only. Under this assumption, the effect of wave and current on entrainment can be isolated for comparison. The mean bed shear stress τ_m under both currents and waves can be obtained following Soulsby (1997). The adapted erosional flux includes the mean bed shear stress in the same manner as (4). By appling this new description of entrainment flux, this model has simplified the computational effort by not including any coupled wave model, but still maintains the key mechanisms of sediment transport in the intertidal areas. The periodic submerging and exposing of intertidal flat accounting for wetting and drying process are solved by nonlinear shallow-water equations.

5.1. Wave-induced bed shear stress and erosional flux over tidal cycle.

The erosional fluxes are considered using the same schematic configuration applied in Roberts et al. (2000) for later qualitative comparison. A plane bed of 0.001 linear slope is considered.over a distance of 6km (origin of the domain is located at the seaward boundary). The seaward boundary is driven by a semidiurnal sinusoidal signal of 5m tidal range. A constant wave height of 0.2m and wave period of 5s are assumed to propagate throughout the domain until depth-limited breaking occurs. Other parameters are given in the table below:

Table 2. Physical parameters for wave-induced bed shear stress

m_e	1×10^{-3}	m/s
D_{50}	0.2	mm
ρ	1027	kg/m^3
$\tau_{s,cr}$	0.2	N/m^2
C_D	2×10^{-3}	
γ	0.5	

The variation of bed shear stress under wave only and the associated erosional fluxes are shown in Fig. 7. For breaking index of 0.5 and small wave incident applied, wave breaking, which corresponds to the maximum bed shear stress, occurs at a small water depth compared to the tidal range. Thus, the bed shear stress at seaward and shoreward reaches its maximum during low tide and high tide, respectively. This behaviour is confirmed with tidal variation as can be seen in Fig. 7b. Seaward, in the lower part of tidal flat, the influence of waves on the bed decreases and the bed shear stress achieve its peaks during low tide level. Shoreward in the upper part, because of the decreasing water depth, the bed shear stress is larger with its maximum at breaking. The shear stress reduces with rising tide as the water depth is large enough to reduce the influence of waves. However, in the shoremost region, the shear stress will achieve its maximum with high tide since the region is within the surf zone during submerging. The bed shear stress for waves also qualitatively agrees with Le Hir et al. (2000) and Roberts et al. (2000). The corresponding erosional flux is shown in Fig. 7a. The maximum erosion is observed at the breaking point. The considered location is inactive (no erosion) once the water depth is large enough so that there is no breaking.

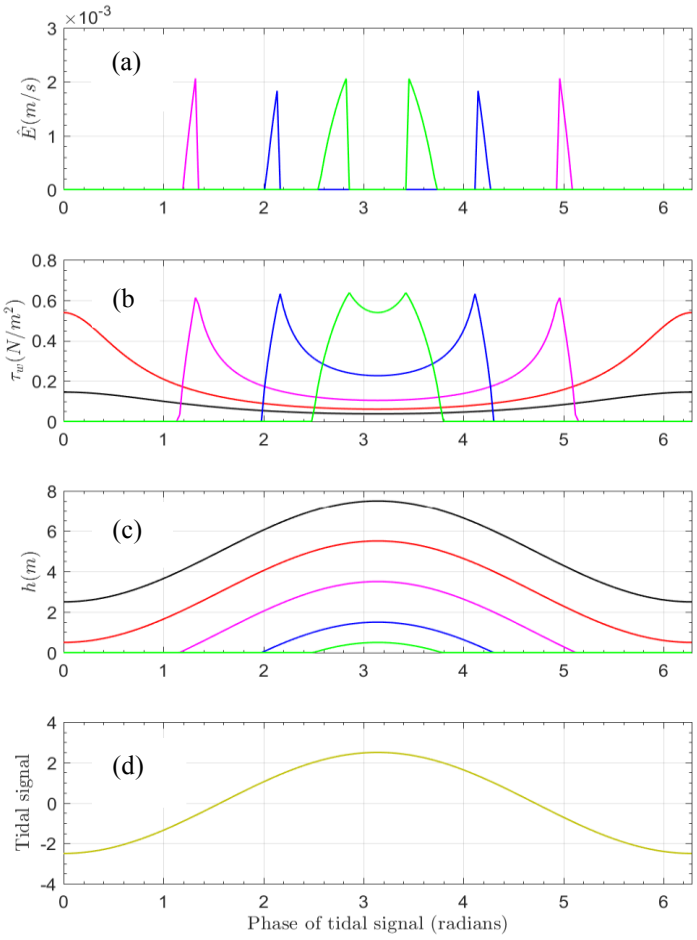

Figure 7. h, τ_w and Q_e at different locations along crosshore over a tidal cycle starting from low tide. The locations are given as distance from offshore boundary ($x = 0$) toward the shoreline: $x = 1$km (black); $x = 3$km (red); $x = 5$km (magenta); $x = 7$km (blue); $x = 8$km (green).

6. Bed change using new erosional flux over tidal cycle

The model has been tested for the configuration bed applied in §4. The physical parameters given in Table 1 are applied in this test (if appropriate). The bed porosity of $p = 0.5$ for fine and medium sand is used. The bed change ΔB over one tidal cycle is shown in Fig. 8. The bed shear stresses and the associated erosional fluxes are shown in Fig. 9. Since we want to investigate the behaviour of the new erosional flux, sediment transport due to suspended-load only is considered. The bed change due to suspended-load under tidal current (see §4.2 for $M = 2\times10^{-4}$) is used for comparison. The behaviour of bed change between those two are quite similar with the tendency of shifting the sediment onshore. Since the new entrainment only occurs within the surf zone, there is no change in bed profile outside the surf zone. Considering the intertidal region, the difference in accretion and erosion between these two are significant. Regarding waves entrainment factor, the accretional and erosional rates are about double the reference result. The contributions of waves into suspended sediment concentration then bed change are notable.

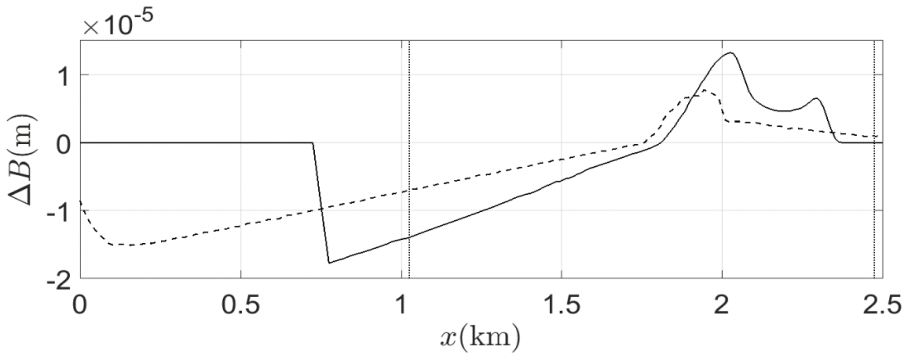

Figure 8. Bed change after one tidal cycle (dashed line: suspended-load only for reference parameters used in §4.1, two dotted lines bound the intertidal region

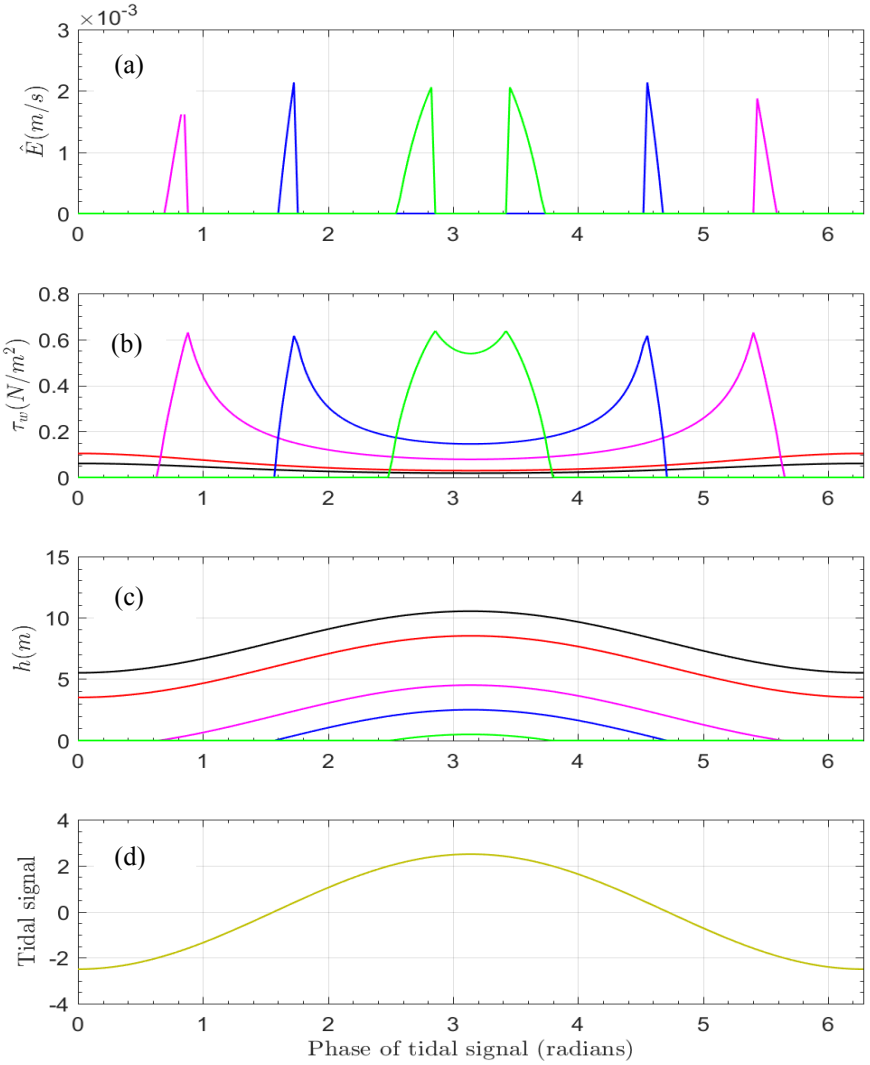

Figure 9. h, τ_w and Q_e at different locations along crosshore over a tidal cycle starting from low tide. The locations are given as distance from offshore boundary ($x = 0$) toward the shoreline: $x = 0.4$km (black); $x = 0.8$km (red); $x = 1.6$km (magenta); $x = 2$km (blue); $x = 2.4$km (green).

7. Conclusion

The relationships between hydrodynamic forcing on two modes of sediment transport (bed-load and suspended-load) on non-cohesive macro-tidal flats have been investigated using coupled hydro-morphodynamic model. In the model, the most important physical processes have been represented in a simplified way. The cross-shore profiles of the flats under tidal currents have been investigated under nonlinear shallow water equations where momentum and friction effects of tidal propagation are included. Individual transport mode and combined mode are considered. The suspended-load transport is more dominant in the accretion of the intertidal region. In the lower part that is always submerged, the bed-load transport becomes more dominant and tends to erode the sediment seaward. The modification on the erosional flux caused by wind-waves has been investigated. It shows that the contribution of waves into suspending sediment then bed change is considerable, even in the configuration of tide-dominated flat.

Further studies of morphodynamics of non-cohesive tidal flats are undertaken. These include: varying tidal range with the inclusion of springs and neaps tides; combination of currents and wavs in erosional flux; the effects of pre-suspended sediment or sediment supply at seaward boundary on the morphodynamics.

Acknowledgements
This research is sponsored by Faculty of Engineering, the University of Nottingham, UK.

References

Anderson, F., 1972. Resuspension of estuarine sediments by small amplitude waves. *Journal of Sediment Petrology,* 42: 602-607.

Carrier, G. and Greenspan, H., 1958. Water waves of finite amplitude on a sloping beach. *Journal of Fluid Mechanics,* 1(4): 97-109.

Eisma, D., 1997. *Intertidal deposits: River mouths, tidal flats and coastal lagoons*. Marine Science Series, CRC Press, Boca Raton.

Friedrichs, C. and Aubrey, D., 1996. Unirform bottom shear stress and equilibrium hypsometry of intertidal flats. *Coastal Estuarine Studies,* 50: 137-170.

Green, M., 2011. Dynamics of very small waves and associated sediment resuspension on an estuarine intertidal flat, *Estuarine Coastal Shelf Science,* 93(4): 449-459.

Green, M., Black, K. and Amos, C., 1997. Control of estuarine sediment dynamics by interactions between currents and waves at several scales, *Marine Geology*, 144: 97-116.

Green, M. and Coco, G., 2013. Review of wave-driven sediment resuspension and transport in estuaries. *Reviews of Geophysics*, 52: 77-117.

Huynh, V., Dodd, N. and Zhu, F., 2017. Morphodynamical modelling using a coordinate transformation method. *Advance in Water Resources (submitted).*

Kirby, R., 2000. Practical implications of tidal flat shape. *Continental Shelf Research,* 20: 1061-1077.

Le Hir, P., Roberts, W., Cazaillet, O., Christie, M., Bassoullet, P. and Bacher, C., 2000. Characterization of intertidal flat hydrodynamics. *Continental Shelf Research,* 20: 1433-1459.

Li, Y. and Mehta, A., 1997. *Mud fluidization by water waves. Cohesive sediment,* Wiley, New York.

Masselink, G. and Short, A., 1993. The effect of tidal range on beach morphodynamics and morphology: A conceptual beach model. Journal of Coastal Research, 9(3): 785-800.

Pritchard, D., Hogg, A. and Roberts, W., 2002. Morphological modelling of intertidal mudflats: the role of cross-shore tidal currents. Continental Shelf Research, 22(11): 1887-1895.

Pritchard, D. and Hogg, A., 2003a. Cross-shore sediment transport and the equilibrium morphology of mudflats under tidal currents. Journal of Geophysical Research, 108(C10): 3313.

Pritchard, D. and Hogg, A., 2003b. On fine sediment transport by long waves in the swash zone of a plane beach. Journal of Fluid Mechanics, 493: 255-275.

Pritchard, D. and Hodd, A., 2005. On the transport of suspended sediment by a swash event on a plane beach. Coastal Engineering, 52: 1-23.

Roberts, W., Le Hir, P. and Whitehouse, R., 2000. Investigation using simple mathematical models of the effect of tidal currents and waves on the profile shape of intertidal mudflats. Continental Shelf Research, 20: 1079-1097.

Short, A., 1991. Macro-meso tidal beach morphodynamics: An overview. Journal of Coastal Research, 7(2): 417-436.

Soulsby, R., 1997. *Dynamics of marine sands: A manual for practical applications.* Thomas Telford, London.